IEEE Control Systems Letters paper presented at
2023 62nd IEEE Conference on Decision and Control (CDC)
December 13-15, 2023. Marina Bay Sands, Singapore

Adaptive Bounded Integral Control With Enhanced Anti-Windup Design

Antonio Russo, Gian Paolo Incremona, Richard Seeber, and Antonella Ferrara

Abstract— **This paper deals with the design of a novel adaptive bounded integral control (BIC) with enhanced anti-windup properties for systems with saturated actuators. Specifically, the BIC is re-designed improving its capability of desaturation after reaching the input bounds. Moreover, by adapting its characteristic curve, the proposed BIC is capable of taking into account time-varying bounds for the actuator saturation. The stability properties of the proposed approach are rigorously analyzed by relying on the Lyapunov theory. Simulation results, carried out by considering the cruising control problem of a platoon of vehicles, are finally shown to assess the proposal.**

Index Terms— **Integral control, bounded-input, anti-windup, adaptive control.**

I. Introduction

Integral control (IC) has proved to be an effective and reliable solution in case of processes characterized by open loop stability, in order to reduce the system sensitivity at null frequency in front of disturbances and parameter variations [1]. Moreover, almost all processes require that the amplitude of the control signal provided by the actuator is limited because of physical or safety reasons. However, combining a saturation with IC has an evident impact on the performances of the saturated systems. In particular, the inattentive design of the controller may "wind-up" the actuator, with consequent possible performance deterioration and instability issues. In fact, the so-called integral windup phenomenon consists of undesired large and poorly decaying overshoots in time intervals during which the control input can no longer affect the controlled variable [2].

A. Brief overview

The actuator saturation problem has been therefore widely addressed in the literature. The most adopted approach, capable of guaranteeing optimality with respect to a predefined cost function, while satisfying input and state constraints, is model predictive control (MPC), see [3] for an overview. However, MPC requires to online solve an optimal control problem, which could be computationally demanding. As an alternative, in the framework of robust control approaches, so-called saturated continuous higher-order sliding mode controllers have been introduced. These are laws characterized by an integral control action, whose output is suitably saturated, while guaranteeing stability and chattering alleviation, see e.g., [4]–[8].

As for the integrator windup phenomenon, instead, in the last decades, many anti-windup approaches, aimed at minimizing the effects caused by saturation, have been proposed in the literature, see [9]–[12], among many works. Such a control problem is relevant in many real-world types of systems, since the lack of anti-windup compensation may lead to poor behaviors of the controlled systems, such as saturation-induced instability issues, see e.g [13], [14] to cite a couple of applications. Therefore, the anti-windup design is not an easy problem to solve and devising numerical and tractable techniques with stability guarantees is still an open challenge (see, e.g., [15], [16] for a further discussion).

More recently, [17] has introduced the concept of the bounded integral control (BIC) algorithm. It consists of an IC capable of generating a control action, which is bounded independently of the plant parameters and states, by projecting the input variable on an ellipsoidal curve. An enhanced version of this algorithm has been then proposed in [18], where a better approximation of the traditional integral action is provided by relaxing some restrictive hypotheses of the original technique. A further extension is finally that in [8], where the BIC is designed as an add-on to almost all higher-order sliding mode controllers aimed at chattering alleviation. Moreover, in [8], the BIC algorithm has been extended to the case of asymmetric saturation limits, and finite-time convergence of the BIC state trajectory towards the BIC characteristic curve has been proved relying on the Lyapunov theory.

B. Contributions with respect to the BIC literature

Making reference to the previously mentioned BIC methods [8], [17], [18], they are characterized by a nonlinear integral control gain, which becomes smaller than one during input saturation to slow down the integration, but it also slowly returns to one during the desaturation phase. As a consequence, such behavior can negatively affect the desired anti-windup compensation, and this spurred us to propose an

This is the final version of the accepted paper submitted to IEEE Control Systems Letters. This work has been partially supported by the European Union under GA no 101101961 - HECATE and by the Italian Ministry for Research in the framework of the 2017 Program for Research Projects of National Interest (PRIN), Grant No. 2017YKXYXJ. Views and opinions expressed are however those of the authors only and do not necessarily reflect those of the European Union or Clean Aviation Joint Undertaking. Neither the European Union nor the granting authority can be held responsible for them. The HECATE project is supported by the Clean Aviation Joint Undertaking and its Members.

A. Russo is with Dipartimento di Ingegneria, Università degli Studi della Campania "Luigi Vanvitelli", 81031 Aversa, Italy (e-mail: *antonio.russo1@unicampania.it*).

G. P. Incremona is with Dipartimento di Elettronica, Informazione e Bioingegneria, Politecnico di Milano, 20133 Milan, Italy (e-mail: *gianpaolo.incremona@polimi.it*).

R. Seeber is with Graz University of Technology, Institute of Automation and Control, Graz, Austria (e-mail: *richard.seeber@tugraz.at*).

A. Ferrara is with the Dipartimento di Ingegneria Industriale e dell'Informazione, University of Pavia, 27100, Pavia, Italy (e-mail: *antonella.ferrara@unipv.it*).

enhanced anti-windup design for a new BIC scheme (see Fig. 1), capable of addressing also the variation over time of the symmetric or asymmetric bounds of the actuator saturation.

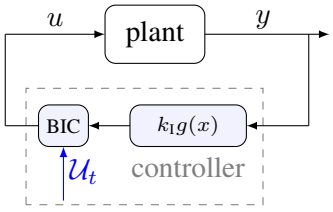

Fig. 1. Adaptive BIC scheme.

Specifically, by comparing the proposed BIC algorithm with [17], the latter introduces a BIC version, which, on the one hand replicates the behavior of the classical IC while saturating the control input, but on the other hand it still partially presents the windup effect due to the time-varying integral gain of the BIC being small during desaturation. In [18] the BIC is similar in terms of anti-windup effects, but it is redesigned to provide a better approximation of the traditional IC in the entire bounded range of the control output and relax the assumption on the selection of the initial conditions of the original BIC. In [8] the BIC is further modified to allow a better approximation of the unitary gain of the IC, considering also asymmetric input bounds, but in analogy with the previous ones the time-varying integral gain of the BIC is small during desaturation.

Moreover, the previous approaches are not capable of adapting in the presence of time-varying bounds, as it is required in different applications, such as the one considered in this paper, that is the cruise control problem for vehicles, where the input forces are bounded depending on the specific properties of tires and on conditions of the road.

II. Problem Formulation

Consider the scheme in Fig. 1, where the plant is a generic nonlinear system

$$\dot{x} = f(x, u), \tag{1}$$

where $x \in \mathcal{X} \subset \mathbb{R}^n$ is the state vector, and $u \in \mathcal{U}_t \subset \mathbb{R}$ is the input, while $\mathcal{U}_t$ is defined as

$$\mathcal{U}_t := [u_{\min}(t), u_{\max}(t)], \tag{2}$$

such that $u_{\min}(t)$, $u_{\max}(t)$ are continuously differentiable time-varying bounds with $u_{\min}(t) < u_{\max}(t)$ for all $t \geq 0$. In the following, for the sake of simplicity, the dependence of all the variables on time will be omitted.

Now, let $g(x) : \mathcal{X} \to \mathbb{R}$ be a scalar function such that the control objective is to regulate $g(x)$ to zero, i.e., to asymptotically stabilize an equilibrium x_e satisfying $g(x_e) = 0$. Having in mind the classical IC, one has that

$$u(t) = \int_0^t k_I g(x(\tau)) \mathrm{d}\tau, \tag{3}$$

with $k_I > 0$ being the integral gain, and such that its dynamics can be rewritten as

$$u = w_1 \tag{4a}$$

$$\dot{w}_1 = k_I g(x). \tag{4b}$$

However, a genuine IC does not guarantee a bounded control signal, thus possibly causing instability issues in combination with actuator saturation. As a solution, the BIC method has been first proposed in [17] and then extended in [8], [18]. More specifically, relying on these previous BIC versions, consider the closed curve in Fig. 2 represented by the following set

$$\mathcal{E} := \left\{ (w_1, w_2) \in \mathbb{R}^2 \ : \ \varepsilon(w_1, w_2) = 0 \right\}, \tag{5}$$

where the expression of $\varepsilon(w_1, w_2)$ is given by

$$\varepsilon(w_1, w_2) := \frac{(w_1 - \bar{u})^{2a}}{\underline{u}^{2a}} + w_2^{2b} - 1 \tag{6}$$

$$\bar{u} := \frac{u_{\max} + u_{\min}}{2}, \quad \underline{u} := \frac{u_{\max} - u_{\min}}{2}, \tag{7}$$

with $a, b \in \mathbb{N}$, being design parameters.

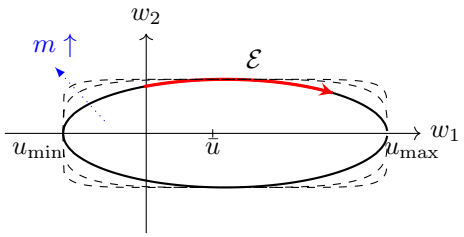

Fig. 2. BIC curves with increasing value of the design parameter m.

A generic BIC formulation, that includes and extends the existing versions of the BIC algorithm, can be written instead as

$$\dot{w}_1 = -k_1 \lfloor \varepsilon \rceil^c (w_1 - \bar{u})^{2a-1} + k_I g(x) w_2^{2b} \tag{8a}$$

$$\dot{w}_2 = -k_I g(x) \frac{w_2}{\underline{u}^{2a}} (w_1 - \bar{u})^{2a-1} - \frac{k_2 \lfloor \varepsilon \rceil^c}{\underline{u}^{2d}} w_2 \tag{8b}$$

where $\lfloor y \rceil^p = \mathrm{sign}\,(y)|y|^p$, $c, d \geq 0$, and k_1 and k_2 are positive scalars to be designed. In particular, the BIC in [17] is obtained when the tuple $(a, b, c, d) = (1, 1, 1, 0)$, $u_{\max} = -u_{\min}$ and $k_1 = 0$. The BIC in [18] is such that $(a, b, c, d) = (1, m, 1, 0)$, $u_{\max} = -u_{\min}$ and $k_1 > 0$, while the BIC in [8] can be defined for any asymmetric bounds by posing the tuple $(a, b, c, d) = (m, m, 0.5, m)$ and $k_1 > 0$. Note that, in [18] and [8] the parameter $m \in \mathbb{N}$, with $m \geq 1$, is such that higher values of m make the integral action very close to the one given by the classical integrator (see Fig. 2). Hence, the BIC working principle is to steer and keep the controller trajectories $w = (w_1, w_2)$ on the curve $\varepsilon(w_1, w_2) = 0$ to emulate a bounded IC action (see [8] and references therein for further details).

In this paper we address the open problem of finding a tractable anti-windup technique based on the BIC approach, by improving the features of the existing algorithms. Moreover, we cope with the case of time-varying input bounds, hence proposing an adaptive version of the BIC method.

III. The Proposed Enhanced Anti-Windup Adaptive BIC

The BIC algorithm presented in this work is designed as

$$u = w_1 \tag{9a}$$

$$\dot{w}_1 = -k_1 \lfloor \varepsilon \rceil^{\frac{1}{2}} (w_1 - \bar{u})^{2m-1} + k_{\mathrm{I}} g(x) \theta(x,w) w_2^{2m} + \dot{\bar{u}} \tag{9b}$$

$$\dot{w}_2 = -k_{\mathrm{I}} g(x) \theta(x,w) \frac{w_2}{\underline{u}^{2m}} (w_1 - \bar{u})^{2m-1} - \frac{k_2 \lfloor \varepsilon \rceil^{\frac{1}{2}}}{\underline{u}^{2m}} w_2 \tag{9c}$$

$$\varepsilon = \frac{(w_1 - \bar{u})^{2m}}{\underline{u}^{2m}} + w_2^{2m} - 1 \tag{9d}$$

with k_1 and k_2 being positive scalars. The term $\theta(x,w)$, which represents one of the novelties with respect to the previous BIC versions, is designed as

$$\theta(x,w) = \begin{cases} \frac{1}{w_2^{2m} + \eta} & \text{if } (w_1 - \bar{u}) g(x) < 0 \,, \\ 1 & \text{otherwise} \,, \end{cases} \tag{9e}$$

with $\eta > 0$ being an arbitrarily small constant. Given that (9e) is discontinuous with respect to x, solutions of (9) are understood in the sense of Filippov [19]. The main idea behind the construction of such a control structure is the following: as long as the BIC state (w_1, w_2) belongs to the closed curve $\mathcal{E}$, then w_1 mimics the classical integral action and, additionally, it is constrained in the interval $(u_{\min}, u_{\max})$. In fact, note that when $(w_1, w_2) \in \mathcal{E}$, the BIC algorithm can take two forms. When $(w_1 - \bar{u}) g(x) \geq 0$, then

$$\dot{w}_1 = k_{\mathrm{I}} g(x) w_2^{2m} + \dot{\bar{u}} \tag{10a}$$

$$\dot{w}_2 = -k_{\mathrm{I}} \frac{g(x)}{\underline{u}^{2m}} w_2 (w_1 - \bar{u})^{2m-1} \,, \tag{10b}$$

else, when $(w_1 - \bar{u}) g(x) < 0$, then

$$\dot{w}_1 = k_{\mathrm{I}} g(x) \frac{w_2^{2m}}{w_2^{2m} + \eta} + \dot{\bar{u}} \tag{11a}$$

$$\dot{w}_2 = -k_{\mathrm{I}} \frac{g(x)}{\underline{u}^{2m}} \frac{w_2 (w_1 - \bar{u})^{2m-1}}{w_2^{2m} + \eta} \,. \tag{11b}$$

The first scenario models the case of the control input moving toward its saturation bounds. Apart from the time-varying term $\dot{\bar{u}}$, the BIC takes the same form as the version presented in [8], with the term w_2^{2m} acting as a nonlinear integral gain that allows to slow down the integration when the control input approaches the saturation bounds. However, in the second case, that is when the control input is moving away from the saturation bounds, the BIC is remodeled as in (11a)–(11b), where the nonlinear integral gain is now $\frac{w_2^{2m}}{w_2^{2m}+\eta}$, which can be approximated with 1 for small values of η, then guaranteeing unitary gain of the integral control during desaturation. Then, the switching term $\theta(x,w)$ allows removing the undesired effect of having a small nonlinear gain w_2^{2m} during desaturation of the control input, with enhanced performance in terms of anti-windup compensation.

A. Stability analysis

The formulation of the BIC as in (10a)–(10b) and (11a)–(11b) depends on the capability of its state (w_1, w_2) to reach the closed curve $\mathcal{E}$. In the next theorem it is proved that, under the following assumption, the BIC state (w_1, w_2) reaches $\mathcal{E}$ in finite time.

$\boldsymbol{\mathcal{A}_1}$: The rate of variation of the input bounds is such that $\dot{u}_{\max} = \dot{u}_{\min}$, i.e., $\underline{u}$ in (7) is constant.

Theorem 1: Given the BIC in (9) with $k_1, k_2, k_{\mathrm{I}} > 0$, if $\boldsymbol{\mathcal{A}_1}$ holds, then the curve (5) with ε in (9d) is almost globally finite time attractive for any input $g(x)$, i.e., for any $(w_1(0), w_2(0)) \in \mathbb{R}^2 \backslash \{(\bar{u}, 0)\}$, there exists $\bar{t}(w_1(0), w_2(0))$ such that the control output u belongs to the compact time-varying interval $[u_{\min}, u_{\max}]$ for all $t \geq \bar{t}(w_1(0), w_2(0))$.

Proof: Consider the state transformation $\xi_1 = w_1 - \bar{u}$, $\xi_2 = w_2$ and the function

$$W(\xi_1, \xi_2) = \varepsilon(\xi_1 + \bar{u}, \xi_2) + 1 = \frac{\xi_1^{2m}}{\underline{u}^{2m}} + \xi_2^{2m} \,, \tag{12}$$

which is positive definite in the (ξ_1, ξ_2) coordinates. Its time derivative, after substituting from (9b)–(9c), is

$$\begin{aligned} \dot{W}(\xi_1, \xi_2) &= \frac{2m}{\underline{u}^{2m}} \xi_1^{2m-1} (\dot{w}_1 - \dot{\bar{u}}) + 2m \xi_2^{2m-1} \dot{w}_2 \\ &= -\frac{2m}{\underline{u}^{2m}} k_1 \lfloor \varepsilon \rceil^{\frac{1}{2}} \xi_1^{2(2m-1)} - \frac{2m}{\underline{u}^{2m}} k_2 \lfloor \varepsilon \rceil^{\frac{1}{2}} \xi_2^{2m} \\ &\quad + k_{\mathrm{I}} g(x) \theta(x,w) \frac{2m}{\underline{u}^{2m}} \xi_2^{2m} \xi_1^{2m-1} + \\ &\quad - k_{\mathrm{I}} g(x) \theta(x,w) \frac{2m}{\underline{u}^{2m}} \xi_2^{2m} \xi_1^{2m-1} + \\ &= -\frac{2m}{\underline{u}^{2m}} \lfloor \varepsilon \rceil^{\frac{1}{2}} \Big(k_1 \xi_1^{2(2m-1)} + k_2 \xi_2^{2m} \Big), \end{aligned} \tag{13}$$

which shows that $\dot{W}(\xi_1, \xi_2)$ is negative definite outside the closed curve $\mathcal{E}$, positive inside and zero on the closed curve $\mathcal{E}$ and at the point $(\xi_1, \xi_2) = (0, 0)$. Since $\varepsilon(w_1, w_2) = W(\xi_1, \xi_2) - 1$, condition $W(\xi_1(0), \xi_2(0)) > 0$ (that is $(w_1(0), w_2(0)) \neq (\bar{u}, 0)$) implies that the parenthesized term in (13) is always positive, which then shows that $W(\xi_1, \xi_2) = 1$ is finite-time attractive by applying [20, Theorem 5.4] using the Lyapunov function $V(\varepsilon) = |\varepsilon|$ with domain of attraction given by $\varepsilon + 1 > 0$, thus making the curve $\mathcal{E}$ almost globally finite time attractive [21, Def. II.1]. ∎

Remark 3.1 (Constant bounds distance): Assumption $\boldsymbol{\mathcal{A}_1}$ can be interpreted as the requirement of keeping the distance between $u_{\min}$ and $u_{\max}$ constant in time, that is the BIC curve in Fig. 2 can move along the w_1 direction but it can neither expand nor shrink. This assumption implies that $\dot{\underline{u}} = 0$, thus allowing an easier computation of the Lyapunov function derivative in Theorem 1.

Remark 3.2 (Switching $\theta(x,w)$): Regarding the switching behavior of $\theta(x,w)$, it is worth noting that the Lyapunov function (12) is a Common Lyapunov Function [22] for all possible values of $\theta(x,w)$, thus stability of the BIC curve is guaranteed for any possible switching sequence of $\theta(x,w)$.

Remark 3.3 (Computation of $\dot{\bar{u}}$): The BIC in (9a)–(9c) requires the knowledge of $\dot{\bar{u}}$ to generate the input u. This term can be either provided by the exogenous system that regulates $u_{\min}$ and $u_{\max}$, or it can be retrieved by ad-hoc differentiators of suitable order, such as, for instance, the so-called Levant's differentiator [23].

B. Illustrative example

In order to appreciate the enhanced anti-windup capabilities of the proposed BIC algorithm compared to the previous versions of the BIC, let us consider the example presented in [17, §V], where a buck-boost converter is taken into account. The dynamics of an ideal buck-boost converter is given by the following nonlinear ODEs

$$\dot{x}_1 = \frac{1}{L}[-(1-u)x_2 + uE] \,, \tag{14}$$

$$\dot{x}_2 = \frac{1}{C}\left[(1-u)x_1 - \frac{x_2}{R}\right] \,, \tag{15}$$

where x_1 and x_2 are the converter current and voltage, respectively, u is the duty cycle and L, C and R are the converter inductance, capacitance and the load resistance, respectively. The control objective is to regulate the converter voltage x_2 to a given reference while keeping the duty cycle constrained in the interval $[0, 0.8]$. The performance of four different integral controllers, i.e., a classical integral controller with saturation, the BIC presented in [17], the BIC presented in [8] and the BIC proposed in this paper are compared. The integral gain is selected equal to 0.35 for all four controllers, while the buck-boost converter parameters are selected as in [17, §V]. Regarding the BIC algorithm presented in [8] and the current proposal, the design parameter m is chosen equal to 20 and all the initial conditions of the BIC controller versions are chosen such that the state (w_1, w_2) belongs to the closed curve.

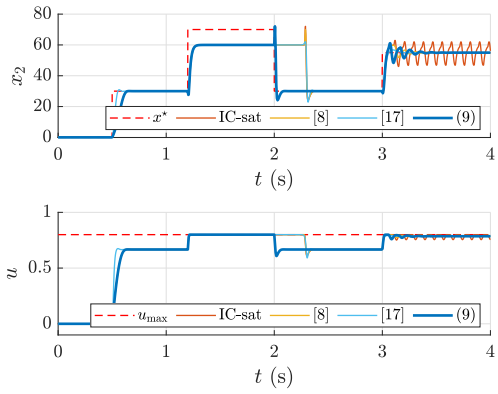

Fig. 3. Anti-windup effects in terms of voltage (top) and duty cycle (bottom) of a buck-boost converter [17, §V], when an IC with saturation, the BIC in [8], the BIC in [17] and the proposal in (9) are applied.

The results of the comparison can be observed in Fig. 3. Initially, the set point for the converter voltage is zero and the duty cycle is kept at zero by all the controllers. At $t = 0.5$ s the reference is set to 30 V, and all the controllers regulate the converter voltage to the desired set-point by controlling the duty cycle to 0.66 approximately. Later, at 1.25 s the set-point is set to 70 V, which is not reachable due to the given input constraint, then all the controllers reach the input bound and saturate. The enhanced anti-windup capabilities can be appreciated at $t = 2$ s, when the set-point is decreased to 30 V and, differently from the previous BIC versions and the classical saturated integral control, the BIC algorithm presented in this work immediately reacts to such a variation. This is the advantage of the proposed approach. Indeed, the classical integrator with saturation, the BIC from [17] and the one from [8] take some time (0.3 s approximately) to desaturate and reach the new set-point. In this time interval, the integrator with saturation shows the classical windup effect, the BIC from [17] slowly desaturates due to the small value of the nonlinear integrator gain, and the BIC from [8] slows down the integration also during desaturation due to the high value of the parameter m (see [8, Remark 3] for further discussion on practices and sensitivity analysis of such a parameter). Finally, at $t = 3$ s the set-point increases to 55 V. While the classical integrator with saturation shows self-sustained oscillations generated by the windup effect, the three different versions of the BIC avoid such phenomenon due to their anti-windup compensation capability.

C. Preservation of the IC stability

In the following, a local stability analysis is introduced to prove that the proposed BIC has the same behavior of the IC around the desired equilibrium point.

Let us consider a slight variation of the BIC algorithm in (9b)–(9c) obtained with $k_1 = 0$, $k_2 > 0$ and the term $\lfloor \varepsilon \rceil^{\frac{1}{2}}$ replaced by a generic function $h(\varepsilon)$, that is

$$\dot{w}_1 = k_{\mathrm{I}} g(x)\theta(x,w) w_2^{2m} + \dot{\bar{u}} \,, \tag{16a}$$

$$\dot{w}_2 = -k_{\mathrm{I}} g(x)\theta(x,w)\frac{w_2}{\underline{u}^{2m}}(w_1 - \bar{u})^{2m-1} - \frac{k_2 h(\varepsilon)}{\underline{u}^{2m}} w_2 \tag{16b}$$

where $h(\cdot)$ is required to have the following properties: $h(0) = 0$, $h(s)\,\mathrm{sign}\,(s) > 0$ for all $s \in \mathbb{R}\backslash\{0\}$, and $\frac{\partial h(s)}{\partial s}|_{s=0} > 0$.

In this section, the following assumption is considered.

$\mathcal{A}_2$: The initial condition of the BIC (16a)–(16b) belongs to $\mathcal{E}\backslash\{(u_{\min}(0), 0), (u_{\max}(0), 0)\}$, with $\mathcal{E}$ in (5) and ε in (9d).

Lemma 2: Consider (16a)–(16b), (9e) with $k_2, k_{\mathrm{I}} > 0$ and assume $\mathcal{A}_1$, $\mathcal{A}_2$ hold. Then, $(w_1(t),\, w_2(t)) \in \mathcal{E}$ for all $t \geq 0$.

Proof: The proof follows from similar reasoning in Theorem 1, where, given $W(\xi_1, \xi_2) = \varepsilon(\xi_1 + \bar{u}, \xi_2) + 1$, it holds that $\dot{W} = -\frac{2m}{\underline{u}^{2m}} h(\varepsilon) k_2 \xi_2^{2m}$. Since $(w_1(0),\, w_2(0)) \in \mathcal{E}$, then $\dot{W} = 0$, i.e., $W(\xi_1(t),\, \xi_2(t)) = W(\xi_1(0),\, \xi_2(0)) = 1$ for all $t > 0$, that is $(w_1(t),\, w_2(t)) \in \mathcal{E}$ for all $t \geq 0$. ■

Note that, due to $\mathcal{A}_2$, $h(\varepsilon)$ will be zero. However, it plays the role of increasing the robustness with respect to external perturbations or computation errors in the dynamics of w_2.

When designing the traditional IC (3) to control nonlinear systems, a local stability analysis is usually performed to select acceptable values (if any) of the gain k_{I} that guarantee asymptotic stability of the closed loop system $\dot{x} = f_{\mathrm{IC}}(x_{\mathrm{IC}})$, with $x_{\mathrm{IC}} = [x^\top, w_1]^\top$. Assuming that f and g are continuously differentiable functions, it is possible to investigate local stability via linearization of the closed-loop system around the equilibrium point $x_{\mathrm{ICe}} = [x_{\mathrm{e}}^\top, w_{1\mathrm{e}}]^\top$ through analysis of the eigenvalues of

$$A_{\mathrm{IC}} = \begin{bmatrix} \frac{\partial f}{\partial x}\big|_{(x_{\mathrm{e}}, w_{1\mathrm{e}})} & \frac{\partial f}{\partial w_1}\big|_{(x_{\mathrm{e}}, w_{1\mathrm{e}})} \\ k_{\mathrm{I}} \frac{\partial g}{\partial x}\big|_{(x_{\mathrm{e}}, w_{1\mathrm{e}})} & 0 \end{bmatrix} \,, \tag{17}$$

where x_{e} is chosen such that $g(x_{\mathrm{e}}) = 0$ and $w_{1\mathrm{e}} \in (u_{\min}, u_{\max})$, with $w_1 = u$. Then, similarly to the result proved in [17], it can be proved that the BIC in (16a)–(16b) inherits the stability properties of the corresponding IC.

Proposition 3: Suppose that the conditions of Lemma 2 hold, that f and g are continuously differentiable, and that the dynamic matrix (17) is Hurwitz. Then, the feedback interconnection of system (1) and that of the BIC formulation (16a)–(16b) with (9e) has an asymptotically stable equilibrium point.

Proof: The equilibrium point $(x_{\mathrm{e}}, w_{1\mathrm{e}})$ of the feedback interconnection of the closed-loop system, comprising of system (1) and the IC, corresponds to an equilibrium $x_{\mathrm{BIC}_e} = [x_{\mathrm{e}}^\top, w_{1\mathrm{e}}, w_{2\mathrm{e}}]^\top$ of the feedback interconnection of system (1) with the BIC (16a)–(16b), where $(w_{1\mathrm{e}}, w_{2\mathrm{e}}) \in \mathcal{E}$, with $\dot{\bar{u}} = 0$. Then, linearizing around x_{BIC_e} leads to the Jacobian (18). Since $h(\varepsilon)$ is required to have positive derivative in zero, then $-k_2 \frac{2m}{\underline{u}^{2m}} w_{2\mathrm{e}}^{2m} \frac{\partial h(\varepsilon)}{\partial \varepsilon}\big|_{(x_{\mathrm{e}}, w_{\mathrm{e}})} < 0$. This in turn implies that eigenvalues of A_{BIC} will have negative real part if the matrix

$$A_{\mathrm{BIC1}} = \begin{bmatrix} \frac{\partial f}{\partial x}\big|_{(x_{\mathrm{e}}, w_{\mathrm{e}})} & \frac{\partial f}{\partial w_1}\big|_{(x_{\mathrm{e}}, w_{\mathrm{e}})} \\ k_{\mathrm{I}} \frac{\partial g}{\partial x}\big|_{(x_{\mathrm{e}}, w_{\mathrm{e}})} \theta(x_e, w_{\mathrm{e}}) w_{2\mathrm{e}}^{2m} & 0 \end{bmatrix}, \quad (19)$$

is Hurwitz. However, since $w_{1e} \in (u_{\min}, u_{\max})$, then $w_{2e} \neq 0$ and $\theta(x_e, w_{\mathrm{e}}) w_{2\mathrm{e}}^{2m} > 0$. This in turn implies that matrix A_{BIC1} is Hurwitz if A_{IC} is Hurwitz. ∎

It is worth noting that, while the BIC version (16a)–(16b) loses the finite time convergence towards $\mathcal{E}$, this alternative version is instrumental to prove that the stability properties of the BIC are inherited from the classical IC. In fact, the local analysis proposed in Proposition 3 is not applicable to the BIC in (9b)–(9c) since it lacks of continuous differentiability at $\varepsilon(w_1, w_2) = 0$ due to the finite time convergence requirement. Some possible choices of $h(\cdot)$ that locally approximate the signed square root function while providing continuous differentiability are e.g., $h(s) = \arctan(s)$ or $h(s) = \tanh(s)$.

IV. A Case Study: Cruise Control Problem

In this section, the proposed BIC is assessed in simulation, considering the cruise control problem for a platoon of N vehicles (see [24, §III.C]) described by

$$\begin{cases} \dot{d}_i(t) = v_{i-1}(t) - v_i(t) \\ m_{\mathrm{v}} \dot{v}_{i-1}(t) = u_{i-1}(t) - F_{\mathrm{L}i-1}(v_{i-1}(t)) \\ m_{\mathrm{v}} \dot{v}_i(t) = u_i(t) - F_{\mathrm{L}i}(v_i(t)) \end{cases}, \ i = 1, \ldots, N, \quad (20)$$

where d_i is the inter-vehicle distance, the 0th vehicle is the platoon leader, and v_i is the ith vehicle velocity. Moreover, m_{v} is the vehicle mass and $F_{\mathrm{L}i}(v_i)$ represents the aerodynamic drag and the rolling resistance forces, described as $F_{\mathrm{L}i}(v_i(t)) = \frac{1}{2}\rho c_{\mathrm{a}} A v_i^2(t) + c_{\mathrm{r}} m_{\mathrm{v}} g_{\mathrm{r}}$, with ρ being the air density, c_{a} the aerodynamic coefficient, A is the equivalent vehicle surface, while c_{r} and g_{r} are the rolling resistance coefficient and the gravitational acceleration, respectively. As for the input force $u_i(t)$, it can be seen as the result of two additive components, representing the traction force component, positive during acceleration and negative during deceleration (regenerative braking), and the mechanical braking force. Such input has to be constrained between two time-varying values depending on the specific properties of tires and on conditions of the road, i.e., $u_i(t) \in [u_{\min}(t), u_{\max}(t)]$ for all $i = 1, \ldots, N$, with $u_{\min} < 0$ and $u_{\max} > 0$ being the force time-varying bounds. Being the torques on the wheels the controlled signals, the assumption that the total force is obtained as the sum of the torques on each wheel is made.

The desired distance among the vehicles is selected according to the Constant Time Headway (CTH) principle requiring the spacing among the cars to be defined as $d_i^{\mathrm{CTH}} = d_{\min} + t_{\mathrm{CTH}} v_i(t)$, for all $i = 1, \ldots, N$.

A. Settings

In the present case study, a platoon of $N = 3$ cars is considered with parameters shown in Table I.

TABLE I
VEHICLES AND BIC PARAMETERS

m_{v}	$c_a\, A$	$d_{\min}$	ρ	t_{CTH}
790 kg	0.88 m^2	4 m	1.22 kg/m^3	3 s
m	k_I	k_1	k_2	η
20	24.17	1	1	10^{-10}

The initial velocities of the three cars are chosen as $[10 \ , 12 \ , 15]^\top$ m/s, while the initial distances are $[110 \ , 130]^\top$ m. The control objective is to regulate the vehicles velocity to a desired reference $v^\star(t)$, that is to take each $g_i(t, v) = v_i(t) - v^\star(t)$ to zero while controlling the inter-vehicle distance to the reference d_i^{CTH}. For each vehicle, the control architecture is made of an internal BIC loop regulating the vehicle velocity and generating the necessary traction force, and an outer PI loop regulating the vehicles distance. The BIC and PI parameters are tuned according to a local stability analysis.

B. Results and discussion

In the considered simulation scenario, starting from their initial velocities and distances, the vehicles reach the desired velocity of 20 m/s and converge to a distance of approximately 64 m (see Fig. 4). During the transient, each vehicle reaches the maximum allowed traction force, which is set to 400 N. As shown in Fig. 5, the BIC correctly saturates and desaturates in the case of constant actuator bound. At $t = 1000$ s, the reference velocity suddenly changes from 20 m/s to 30 m/s. In order to allow reaching such velocity reference,

$$A_{\mathrm{BIC}} = \begin{bmatrix} \frac{\partial f}{\partial x}\big|_{(x_{\mathrm{e}}, w_{\mathrm{e}})} & \frac{\partial f}{\partial w_1}\big|_{(x_{\mathrm{e}}, w_{\mathrm{e}})} & 0 \\ k_{\mathrm{I}} \frac{\partial g}{\partial x}\big|_{(x_{\mathrm{e}}, w_{\mathrm{e}})} \theta(x_e, w_{\mathrm{e}}) w_{2\mathrm{e}}^{2m} & 0 & 0 \\ -k_{\mathrm{I}} \frac{\partial g}{\partial x}\big|_{(x_{\mathrm{e}}, w_{\mathrm{e}})} \theta(x_e, w_{\mathrm{e}}) \frac{w_{2\mathrm{e}}}{\underline{u}^{2m}} (w_{1\mathrm{e}} - \bar{u}) & -k_2 \frac{\partial h(\varepsilon)}{\partial w_1}\big|_{(x_{\mathrm{e}}, w_{\mathrm{e}})} w_{2\mathrm{e}} & -k_2 \frac{2m}{\underline{u}^{2m}} w_{2\mathrm{e}}^{2m} \frac{\partial h(\varepsilon)}{\partial \varepsilon}\big|_{(x_{\mathrm{e}}, w_{\mathrm{e}})} \end{bmatrix} \quad (18)$$

the cruise control system smoothly changes the maximum allowed traction force to 650 N following a ramp profile. As shown in Fig. 5, the vehicles actuators saturate during the actuator bound variation. Nevertheless, the designed BIC algorithm correctly deals with the time-varying actuator bounds, and the velocity reference is correctly reached. Fig. 6 shows how the BIC state moves along the adaptive BIC curves which translates from an initial configuration with $u_{\max} = -u_{\min} = 400$ to $u_{\max} = 650$ and $u_{\min} = -150$.

V. Conclusions

In this paper, a novel BIC algorithm is proposed for saturated systems. In order to avoid a slow desaturation phase, which affects the previous versions of this algorithm, the BIC gain is suitably modified to speed up the reaching of the unitary integral gain. Moreover, if time-varying bounds for the actuator saturation are required, the proposed BIC characteristic curve is adapted over time. The theoretical analysis reported in this paper provides conditions for the attractiveness of the BIC characteristic curve and the fulfillment of the input bounds. The proposed BIC approach provides satisfactory performance, as finally assessed in simulation relying on a cruise control problem for a platoon of vehicles.

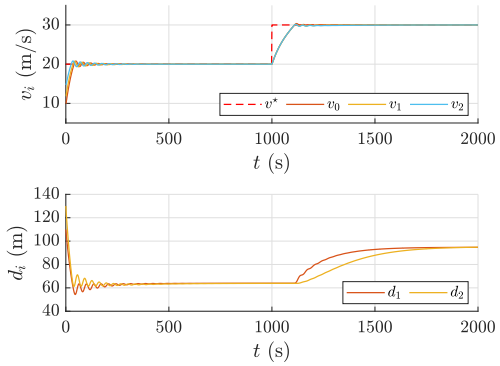

Fig. 4. Velocity profiles (top) and distances between the vehicles (bottom).

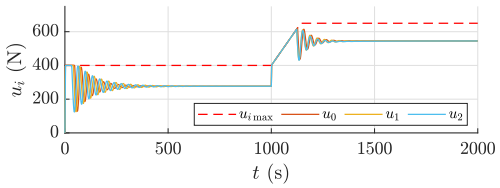

Fig. 5. Input force profiles with time-varying bounds.

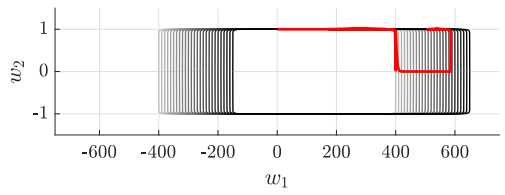

Fig. 6. BIC state space $\{w_1, w_2\}$ and time-varying characteristic curves.

References

[1] G. C. Goodwin, S. F. Graebe, and M. E. Salgado, *Control System Design*. Upper Saddle River: Prentice Hall, 2000.

[2] P. Hippe, *Windup in Control: Its Effects and Their Prevention*. London: Springer-Verlag, 2006.

[3] D. Q. Mayne, "Model predictive control: recent developments and future promise," *Automatica*, vol. 50, no. 12, pp. 2967–2986, 2014.

[4] A. Ferrara and M. Rubagotti, "A sub-optimal second order sliding mode controller for systems with saturating actuators," *IEEE Transactions on Automatic Control*, vol. 54, no. 5, pp. 1082–1087, 2009.

[5] G. P. Incremona, M. Rubagotti, and A. Ferrara, "Sliding mode control of constrained nonlinear systems," *IEEE Transactions on Automatic Control*, vol. 62, no. 6, pp. 2965–2972, 2017.

[6] R. Seeber and M. Horn, "Guaranteeing disturbance rejection and control signal continuity for the saturated super-twisting algorithm," *IEEE Control Systems Letters*, vol. 3, no. 3, pp. 715–720, 2019.

[7] R. Seeber and M. Reichhartinger, "Conditioned super-twisting algorithm for systems with saturated control action," *Automatica*, vol. 116, p. 108921, 2020.

[8] A. Russo, G. P. Incremona, and A. Cavallo, "Higher-order sliding mode design with bounded integral control generation," *Automatica*, vol. 143, p. 110430, 2022.

[9] Z. Lin, A. Saberi, and A. Stoorvogel, "Semiglobal stabilization of linear discrete-time systems subject to input saturation, via linear feedback-an are-based approach," *IEEE Transactions on Automatic Control*, vol. 41, no. 8, pp. 1203–1207, 1996.

[10] A. Saberi, Z. Lin, and A. Teel, "Control of linear systems with saturating actuators," *IEEE Transactions on Automatic Control*, vol. 41, no. 3, pp. 368–378, 1996.

[11] D. Henrion, S. Tarbouriech, and G. Garcia, "Output feedback robust stabilization of uncertain linear systems with saturating controls: an lmi approach," *IEEE Transactions on Automatic Control*, vol. 44, no. 11, pp. 2230–2237, 1999.

[12] F. Wu, K. M. Grigoriadis, and A. Packard, "Anti-windup controller design using linear parameter-varying control methods," *International Journal of Control*, vol. 73, no. 12, pp. 1104–1114, 2000.

[13] N. O. Perez-Arancibia, T.-C. Tsao, and J. S. Gibson, "Saturation-induced instability and its avoidance in adaptive control of hard disk drives," *IEEE Transactions on Control Systems Technology*, vol. 18, no. 2, pp. 368–382, 2010.

[14] L. Dritsas, E. Kontouras, I. Kitsios, and A. Tzes, "Aggressive control design for electric power generation plants," in *26th Mediterranean Conference on Control and Automation*, Zadar, Croatia, Jun. 2018, pp. 667–672.

[15] S. Tarbouriech and M. Turner, "Anti-windup design: an overview of some recent advances and open problems," *IET Control Theory & Applications*, vol. 3, pp. 1–19, 2009.

[16] M. Oliveira, J. Gomes da Silva, D. Coutinho, and S. Tarbouriech, "Anti-windup design for a class of nonlinear control systems," *IFAC Proceedings Volumes*, vol. 44, no. 1, pp. 13 432–13 437, 2011, 18th IFAC World Congress.

[17] G. C. Konstantopoulos, Q.-C. Zhong, B. Ren, and M. Krstic, "Bounded integral control of input-to-state practically stable nonlinear systems to guarantee closed-loop stability," *IEEE Transactions on Automatic Control*, vol. 61, no. 12, pp. 4196–4202, 2016.

[18] G. C. Konstantopoulos, "Enhanced bounded integral control of input-to-state stable nonlinear systems," *IFAC-PapersOnLine*, vol. 50, no. 1, pp. 8151–8156, Jul. 2017, 20th IFAC World Congress.

[19] A. F. Filippov, *Differential Equations with Discontinuous Right-Hand Side*. Dordrecht, The Netherlands: Kluwer Academic Publishing, 1988.

[20] A. Bacciotti and L. Rosier, *Liapunov Functions and Stability in Control Theory*. Berlin, Heidelberg: Springer, 2010.

[21] P. Monzón, "On necessary conditions for almost global stability," *IEEE Transactions on Automatic Control*, vol. 48, no. 4, pp. 631–634, 2003.

[22] D. Liberzon, *Switching in Systems and Control*, ser. Systems & Control: Foundations & Applications. Boston: Birkhäuser, 2003.

[23] A. Levant, "Higher-order sliding modes, differentiation and output-feedback control," *International Journal of Control*, vol. 76, no. 9–10, pp. 924–941, 2003.

[24] A. Ferrara, G. P. Incremona, E. Birliba, and P. Goatin, "Multi-scale model-based hierarchical control of freeway traffic via platoons of connected and automated vehicles," *IEEE Open Journal of Intelligent Transportation Systems*, vol. 3, pp. 799–812, 2022.